

Laboratory Investigations of Deep-Water Wave Transformation and Stability

**Piotr Wilde, Eugeniusz Sobierajski, Włodzimierz Chybicki,
Łukasz Sobczak**

Institute of Hydro-Engineering of the Polish Academy of Sciences,
ul. Kościarska 7, 80-953 Gdańsk, Poland, e-mail: p_wilde@ibwpan.gda.pl

(Received February 28, 2002; revised October 01, 2003)

Abstract

The authors performed laboratory investigations and the analysis of the transformation of deep-water waves in the flume of the Institute of Hydro-Engineering. Special wave trains were generated by our piston-type wavemaker. Due to the transformation the wave profiles changed along the path of propagation. At first, the changes appeared at the ends of the wave train. Far from the generator they intruded into the middle interval of initially regular waves. Finally, the whole wave train consisted of a set of irregular groups. To study the instability problem the wave trains were modulated by superposition of wave groups with very small amplitudes. The number of waves in a group was a very important parameter. When the number was proper, even small amplitudes of modulation resulted in strong development of amplitudes of wave groups. In our theoretical analysis the non-linear Schroedinger equation was used. The comparison of laboratory and theoretical results proved that this equation is useful but it does not describe the phenomenon in the best way. There have been many attempts to construct a numerical procedure that describes the propagation of water waves. Very often the numerical algorithm is not stable and the results of calculation diverge from the expected behaviour. The authors believe that in many cases the instability is due to the physical loss of stability of the wave train and thus it is necessary to have a good understanding of the physics of the studied motion.

Key words: water waves, stability, transformation, laboratory investigation

1. Introduction

The new, very precisely shaped, wave flume of the Institute of Hydro-Engineering is 64 m long, 0.6 m wide and the height is 1.40 m. It has a programmable piston type generator. During the first experiments in the new facility Sobierajski (1999) tested the wave processes by measuring the wave profiles along the flume. In Fig. 1 parts of measured piston motion and generated deep water waves are shown with the corresponding amplitudes of Fourier series. The first graph corresponds to the time series of horizontal displacements of the piston and represents a cosine

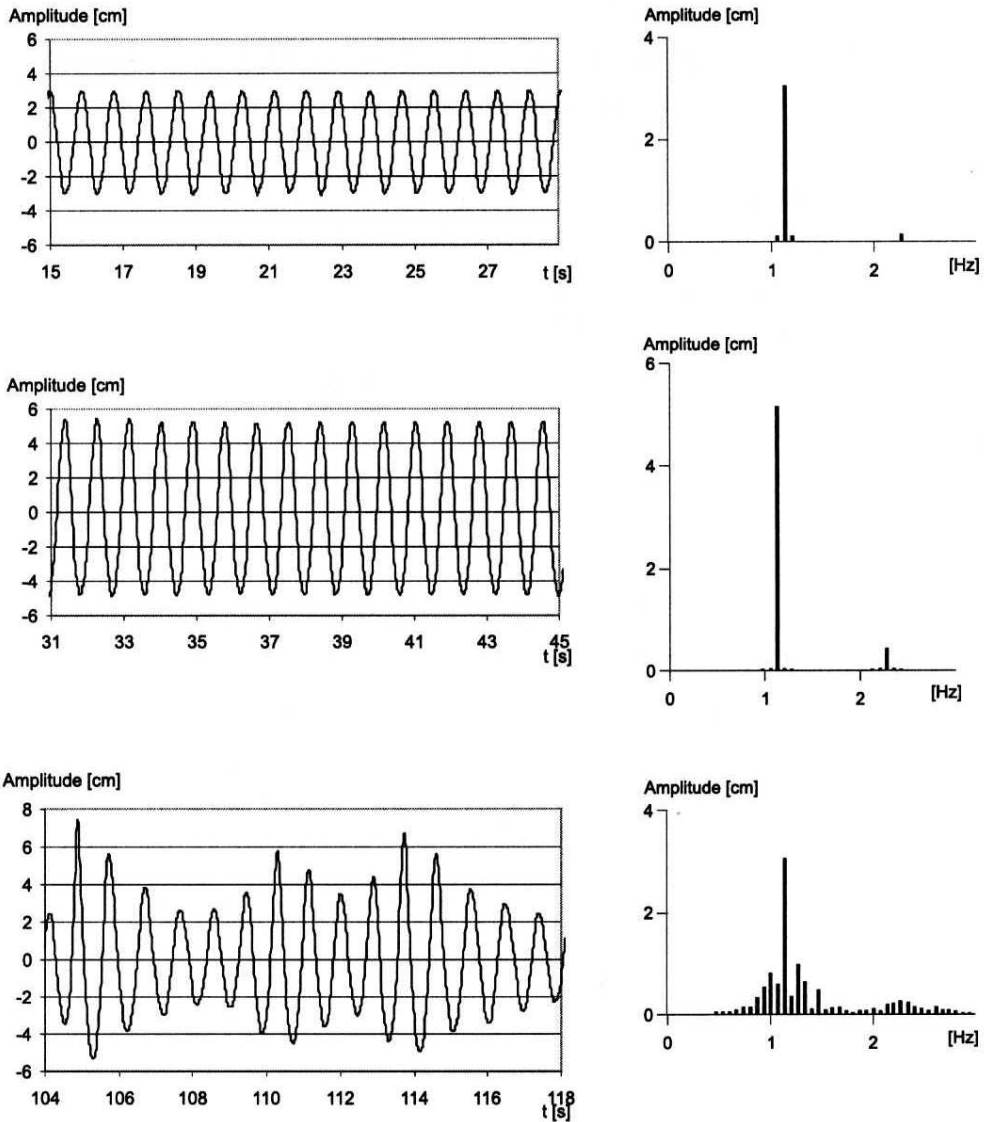


Fig. 1. Samples of the recorded wavemaker's motion ($L_l = 1.20$, $h = 0.6$, $L_l/h = 2$) and wave profiles recorded along the flume (at $x = 7L_l$ and $x = 40L_l$) with related amplitudes of the Fourier components

curve with one component in the corresponding spectral density. The surface elevation in the neighbourhood of the generator is depicted in the second graph and corresponds to a standard Stokes wave with two significant components. The third graph shows the measured time series of surface elevation far from the generator. Irregular wave groups appear in the experimental time series and the corresponding spectral density has many components. The regular waves became unstable. The aim of the experiments performed in the year 2001 was to study the transformation and stability of the waves.

The water waves are dispersive, which means that the speed of propagation of monochromatic waves depends upon their frequency. The properties of dispersive and non-dispersive waves are described and discussed by Witham (1974). Lighthill (1965) was one of the first to study the transformation of non-linear deep-water waves along their ways of propagation. His analysis led to the conclusion that the regular wave is not always stable and there is a region of instability. Often the stability criteria and the corresponding instability regions carry the name "Lighthill".

Three-dimensional ocean waves are complicated and it is not easy to study their properties. Two dimensional water waves generated in a wave flume are much simpler and easier to describe by methods of applied mathematics. The deep-water waves are the easiest cases, their description is comparatively simple. To study the non-linear behaviour and to describe within the standard continuum theory of hydrodynamics, one has to investigate waves that do not break but are close to breaking. For short (deep water) non breaking waves the component with the double frequency is about 5% to 10% of the first one. Thus it is possible to reduce the problem to a two-dimensional description (one dimension in space x and one in time t) and the behaviour may be described by a two-dimensional partial differential equation. The starting point of such descriptions is the dispersion equation that relates the angular frequency to the wave number and the amplitude of a monochromatic wave.

Benjamin and Feir (1962) demonstrated that a regular continuous deep-water wave might be unstable to modulations of its envelope. The standard method of stability analysis of motion was used. Infinitesimal perturbations are considered and their growth indicates instability. In the next paper Benjamin (1967) presented a generalisation. Zacharov 1968 and independently Hasimoto and Ono (1972) showed that the stability problem might be described by the non-linear Schroedinger differential equation. This equation is very useful in the study of soliton behaviour and therefore it is very useful in descriptions of large modulations that are found in experiments.

The initial condition corresponds to water at rest. The piston of the wave generator starts to move with initial zero velocity and zero acceleration. The amplitude grows slowly in time. Finally the prescribed asymptotic value is reached and kept constant and then a decay interval is attached, such that the decrease

of amplitude is slow and smooth. Wilde and Wilde (2001) describe the details in their paper. The suitable time series is calculated on a computer and fed into the control system of the generator. The transformation of wave trains generated in such way was investigated along the flume in experiments and compared with a theoretical solution.

In the standard instability theory infinitesimal perturbations are considered. Usually small sinusoidal displacements are introduced in the control time series and the changes due to the modulations are calculated along the path of propagation of the wave. We applied such a method in our experiments. After the stability was lost the modulations grew to large amplitudes. We studied such transformations extensively.

The phenomenon of wave groups is still investigated. For example Chereskin and Mollo-Christensen (1985), Shemer et al (1988) and Stansberg (1992) consider the development of non-linear wave groups. Now the experimental facilities are much better and developments in computers make extensive data processing and analysis easier.

2. Description of Experiments

In the experiments the water depth was $h = 0.60$ m. The changes in surface elevations were measured at fixed points by wave gauges as functions of time. In the experiments the sampling frequency was 50 Hz. Seven gauges were placed in the flume in several different schemes. The details are described in an internal report. In this paper the described results correspond mainly to the below-specified scheme. The first gauge was placed at 4 m and the second at 8 m in front of the piston at rest. Five consecutive gauges were placed at distances equal to multiples of 8 m from the second one. Thus the distance from the position of the piston at rest to the last gauge was 48 m. The consecutive gauges and their positions were denoted by the symbols S1, S2, ... up to the last one, S7, in a scheme.

The motion (not modulated) of the piston was fixed by a calculated time series fed into the control time series of the generator, which had an interval of growth (5 wave periods) a regular interval (35 wave period) and an interval of decay (8 wave periods). Such a form of wave trains was chosen to obtain smooth transition to the regular interval. The measurements at the consecutive gauges showed that spreading of changes from the intervals of growth and decay into the internal zone of wave train was observed.

To study the stability problem, initial modulations of the control time series of piston motion were introduced in the form of wave groups. Experiments were repeated for the following ratios of amplitudes of modulations a_m to the amplitude of the regular wave a_0 : $a_m/a_0 = [0.00, 0.05, 0.10, 0.15, 0.20, 0.30]$, and for the following numbers of waves in a group: $n_T = [4.00, 4.50, 5.00, 5.36, 6.00, 7.00]$ where n_T is the number of waves in a group in time. In these experiments the

interval of growth had 9 wave periods, the interval of regular waves had 86 and the interval of decay had 12 in the control time series for piston motion. The experiments with the non modulated time series showed that the reflection was negligible and thus it was possible to extend the length of the wave train.

3. Basic Theoretical Relations

The basis of the analysis is the dispersion relation for the Stokes wave within the third order of approximation, as given in many textbooks. For example, the formula given in Werhausen & Laitone (1960) taken from a report by Skjelbreia (1959) is:

$$\omega_0^2 = gk_0 \tanh k_0 h \left(1 + a_0^2 k_0^2 \frac{8 + \cosh 4k_0 h}{8 \sinh^4 k_0 h} + \dots \right), \quad (1)$$

where ω_0 is the angular frequency of the regular non-linear wave, $k_0 = 2\pi/L_0$, k_0 is the wave number and L_0 the wavelength, h is the depth of the water, g the acceleration in the gravity field and a_0 is the amplitude of the first harmonic. It should be stressed that in the analysis it is assumed that the amplitudes are small. The relation (1) may be expressed in terms of the following dimensionless parameters: $k_0 h$, $k_0 a_0$ and $\omega_0^2/(gk_0)$. When $K = 2\pi/(n_L L)$ it may be assumed that the water is deep and the following simplified dispersion relation may be used

$$\omega_0^2 = gk_0 \left(1 + a_0^2 k_0^2 + \dots \right). \quad (2)$$

If the amplitude a_0 is so small that $k_0 a_0 \ll 1$ it is sufficient to take into account two terms of the expansion and to neglect the higher order terms denoted in (2) by the three dots.

In the standard stability analysis of non-linear waves the dispersion relation may be expressed by a Taylor series expansion around the linear solution that corresponds to the case $a_l \rightarrow 0$, $\omega \rightarrow \omega_l$ and $k \rightarrow k_l$. The following relation gives such an expansion.

$$\omega - \omega_l = v_g (k - k_l) + \alpha (k - k_l)^2 + \beta (a^2 - a_l^2), \quad (3)$$

where $v_g = \partial\omega/\partial k$ is the group velocity, $\alpha = 0.5\partial^2\omega/\partial k^2$ and $\beta = \partial\omega/\partial(a^2)$ calculated at $a = 0$, $\omega = \omega_l$ and $k = k_l$. For the linear case of deep water waves according to Eq. (2) $\omega_l = \sqrt{gk_l}$ and the coefficients in the expansion (3) are

$$v_g = \frac{g}{2\omega_l} = \frac{\omega_l}{2k_l}, \quad \alpha = -\frac{\omega_l}{8k_l^2}, \quad \beta = \frac{1}{2}\omega_l k_l^2. \quad (4)$$

The equation (3) is the basis for the construction of the corresponding non-linear Schroedinger equation as given in the paper by Yuen and Lake (1982), namely

$$i(A_{,t} + v_g A_{,x}) + \alpha A_{,xx} - \beta |A|^2 A = 0, \quad (5)$$

where $A(x, t) = a(x, t) \exp[i\theta(x, t)]$ is the complex amplitude and $a(x, t)$ is the modulus, $\theta(x, t)$ is the phase and the subscripts t and x denote the derivatives with respect to time t and x . The complex amplitude is defined in such a way that the complex function

$$Z(x, t) = A(x, t) \exp[i(k_1 x - \omega_1 t)], \quad (6)$$

corresponds exactly to the first term in the description of a regular Stokes wave. Thus it follows

$$A(x, t) = a_0 \exp\{i[(k_0 - k_1)x - (\omega_0 - \omega_1)t]\}. \quad (7)$$

It is easy to verify that the substitution of this relation into the differential equation (5) leads to the following relation

$$(\omega_0 - \omega_1) - v_g(k_0 - k_1) - \alpha(k_0 - k_1)^2 - \beta a_0^2 = 0.$$

This expression corresponds exactly to the dispersion relation (3).

For a regular Stokes wave the dispersion relation is an equation that fixes the angular frequency if the wave number and the amplitude are known. Let us call a wave number controlled test when $k_0 = k_1$. For this case it follows from the dispersion relation (3) that

$$\omega_0 - \omega_1 = \beta a_0^2 = \frac{1}{2} \omega_1 k_1^2 a_0^2, \quad (8)$$

and the complex amplitude for the regular wave train is given by

$$A(x, t) = a_0 \exp\left(-i \frac{1}{2} k_1^2 a_0^2 \omega_1 t\right) = a_0 \exp(-i\beta t). \quad (9)$$

This is the standard case studied in theoretical consideration.

In our laboratory tests the piston motion is prescribed as a function of time and this corresponds to a frequency controlled test. Thus we assume that $\omega_0 = \omega_1$ and the value of $k_0 - k_1$ has to be calculated from the dispersion relation (3). The solution of the second order algebraic equation yields

$$k_0 - k_1 = -2k_1 \left[1 - \sqrt{1 - k_1^2 a_0^2}\right] \approx -k_1^3 a_0^2 \quad (10)$$

where the last term is obtained from a binomial expansion and is a good approximation.

It follows that the approximated complex amplitude in the frequency-controlled test is

$$A(x, t) = a_0 \exp(-ik_1^3 a_0^2 x). \quad (11)$$

If the exact expression in (10) is used for the complex amplitude then the Schroedinger equation is exactly satisfied. If the approximated expression (10) is used, terms with higher powers of the amplitude have to be neglected. Substitution of $x = v_g t$ into the expression (11) leads to the relation (9). Thus both expressions are the same when the distance x is replaced by the product of time with the group velocity. It must be stressed however, that this similarity follows from the binomial expansion in the relation (10), which is true for very small values of the amplitude.

Let us assume that the complex amplitude in the wave number controlled test, given by the relation (9), is changed by the addition of functions with infinitesimal amplitudes ε_+ , ε_- according to the formula

$$A(x, t) = \{a_0 + \exp(Vt) [\varepsilon_+ \exp(iK\xi) + \varepsilon_- \exp(-iK\xi)]\} \exp(-i\beta t), \quad (12)$$

where $\xi = x - v_g t$, V with dimensions 1/s is a constant, K with dimension 1/m is the wave number of the group $K = 2\pi/(n_L L)$ and where n_L (not necessary an integer) is the number of wavelengths in the group considered in space. This expression is obtained as a superposition of infinitesimal modifications on large displacements corresponding to the second order Stokes wave. The amplitudes of the disturbances and the value of the dimensionless quantity Vt have to be very small. Thus the value of $\exp(Vt)$ is very close to the value of the function $1 + Vt$.

Upon differentiation of the expression (12) and substitution into the Schroedinger differential equation, a complex number relation is obtained, that corresponds to the following set of two real homogeneous equations

$$\begin{bmatrix} \left(\frac{\omega_l}{8k_l^2} K^2 - k_l^2 a_0^2 \omega_l \right) \cos K(x - v_g t) & -V \sin K(x - v_g t) \\ V \cos K(x - v_g t) & \frac{\omega_l}{8k_l^2} K^2 \sin K(x - v_g t) \end{bmatrix} \times \begin{bmatrix} \varepsilon_+ + \varepsilon_- \\ \varepsilon_+ - \varepsilon_- \end{bmatrix} = \begin{bmatrix} 0 \\ 0 \end{bmatrix}. \quad (13)$$

A non-trivial solution exists if the determinant of the equation is zero. Then we obtain

$$\frac{V^2}{\omega_l^2} = \left[k_l^2 a_0^2 - \frac{K^2}{8k_l^2} \right] \frac{K^2}{8k_l^2}. \quad (14)$$

The unknown coefficient V is real if the value of K is in the interval

$$0 < K/k_l < 2\sqrt{2}k_l a_0. \quad (15)$$

This is the interval of instability as the disturbances grow in time according to the expression (12).

The maximum value of V/ω_l is

$$\left(\frac{V}{\omega_l}\right)_{\max} = \frac{1}{2}k_l^2 a_0^2, \quad (16)$$

and corresponds to the value of K/k_l given by the relation

$$(K/k_l)_m = 2k_l a_0. \quad (17)$$

The relations (14)–(17) are standard expressions for the stability criterion.

In our experiments we control the motion of the generator as a function of time based on the assumed frequency. Thus we have a frequency controlled experiment. In this case the solution with the infinitesimal, superposed modifications (as in the case of wave number controlled experiment (12)) may assume the form

$$A(x, t) = \{a_0 + (1 + Ux) [\varepsilon_+ \exp(iK\xi) + \varepsilon_- \exp(-iK\xi)]\} \exp(-ik_l^3 a_0^2 x) \quad (18)$$

where U is an unknown parameter with dimension $1/m$.

Upon differentiation of the expression (12), substitution into the Schroedinger differential equation and neglecting terms with higher order terms in $k_l a_0$, a complex number relation is obtained, which corresponds to the following set of two real homogeneous equations

$$\begin{bmatrix} \left(\frac{K^2}{8k_l^2} - k_l^2 a_0^2\right) \cos K(x - v_g t) & -\frac{U}{2k_l} \sin K(x - v_g t) \\ \frac{U}{2k_l} \cos K(x - v_g t) & \frac{K^2}{8k_l^2} \sin K(x - v_g t) \end{bmatrix} \times \quad (19)$$

$$\times \begin{bmatrix} \varepsilon_+ + \varepsilon_- \\ \varepsilon_+ - \varepsilon_- \end{bmatrix} = \begin{bmatrix} 0 \\ 0 \end{bmatrix}.$$

A non-trivial solution exists if the determinant of the equation is zero. Thus we obtain

$$\frac{U^2}{4k_l^2} = \left[k_l^2 a_0^2 - \frac{K^2}{8k_l^2} \right] \frac{K^2}{8k_l^2}. \quad (20)$$

Comparison of the expression (14) with (20) shows that $V/U = \omega_l/(2k_l) = v_g$. The ratio is equal to the group velocity.

The functions $U/(2k_l)$ as functions of K/k_l and parameters $k_l a_0$ are plotted in Fig. 2, where four curves correspond to four dimensionless numbers $k_l a_0 = [0.2356, 0.2094, 0.1833, 0.1571]$. The intervals of stability depend upon the values of $k_l a_0$ by the relation (15). When the value of $k_l a_0$ increases the length of the interval and the maximum value of $U/(2k_l)$ increase. This is the standard illustration of the stability criterion. In planing the experiments it is convenient to change the independent variable. The functions $U/(2k_l)$ as functions of $2k_l/K$ and

parameters ka_0 are depicted in Fig. 3. The dimensionless numbers $2k_l/K$ correspond to the number of waves in a group in time n_T (twice the number in space). This graph shows directly how the deep water wave with a prescribed amplitude is sensitive to the number of waves in a modification.

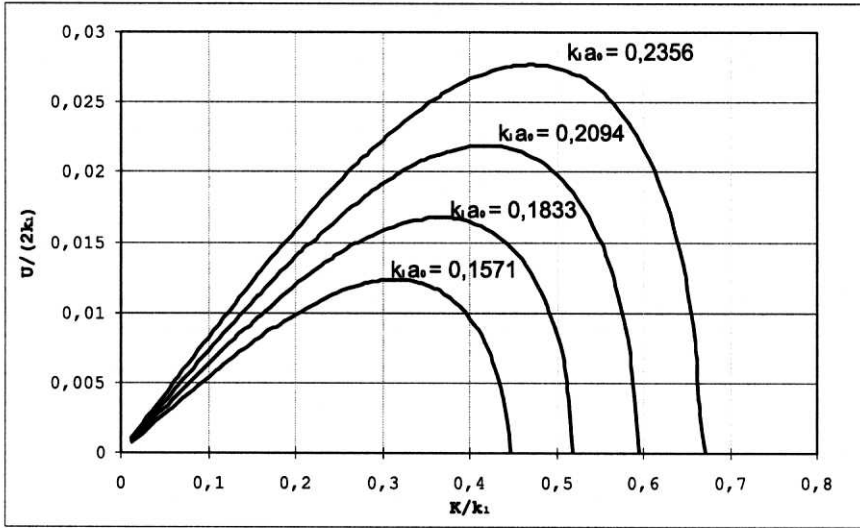


Fig. 2. $U/(2k_l)$ as a function of K/k_l

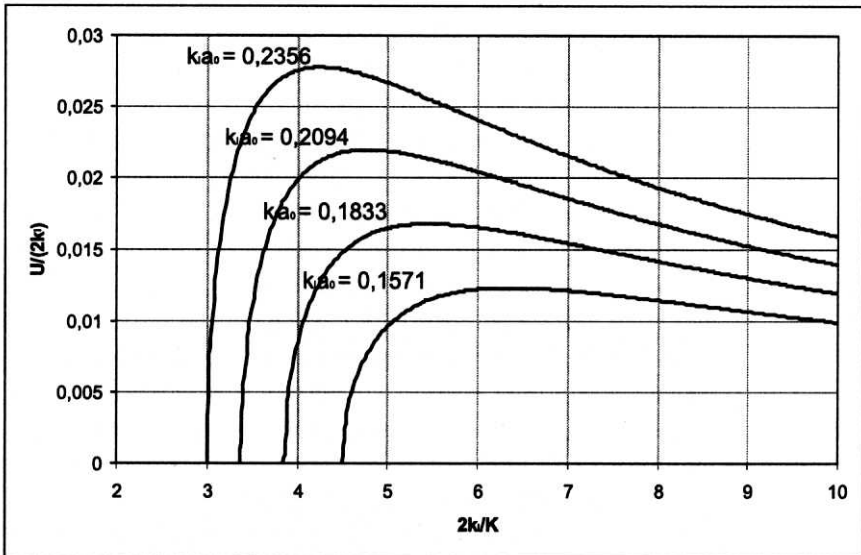


Fig. 3. $U(2k)$ as functions of $2k_l/k$

To obtain an expression for the surface elevation in the modified case one has to multiply the complex amplitude given by the relation (18) by $\exp[i(k_l x - \omega_l t)]$. It follows finally that

$$Z(x, t) = a_0 \exp[i(k_0 x - \omega_l t)] + (1 + Ux) \varepsilon_+ \exp\{i[(k_0 + K)x - (\omega_l + \varpi_l/n_T)t]\} + (1 + Ux) \varepsilon_- \exp\{i[(k_0 - K)x - (\omega_l - \varpi_l/n_T)t]\}, \quad (21)$$

where $n_T = 2k_l/K$ is the number of waves in a group in time.

4. The Analysis of the Experimental Wave Transformation

The new wave flume has a piston type generator that is not very suitable for the generation of deep-water waves. The waves discussed in this paper had a period equal to 0.878 s, which corresponds in the linear dispersion formula to wavelength equal to 1.20 m (depth $h = 0.6$ m). Thus the length of the non-linear wave, depending on the amplitude, is slightly longer. It is assumed that at a distance of 4 m from the position of the piston the transformation into the deep water case is completed and the measured wave at $S1$ may be considered to be a reference wave.

The measurements of surface elevations for a long wave train with an almost perfect interval of regular waves and comparatively short intervals of growth and decay are depicted in Fig. 4. For these and the following curves when not directly stated, the dimensionless parameter $k_l a_0$ is equal to 0.196. The wave amplitude a_0 is half the mean wave height in the regular interval as measured at gauge $S2$. Changes along the flume in all three intervals can be observed. The diagrams for the consecutive gauges are shifted in time by the group velocity that corresponds to the speed of propagation of energy. The reference wave is the one measured at gauge $S1$. It is similar to the diagram for piston motion. The measured surface elevation at $S2$ (4 m from the reference gauge) is similar and substantial differences are only in the intervals of growth and decay. The waves move with phase velocity while the energy moves with group velocity. Thus in these intervals the waves propagate faster and there is no energy supply. The result is that the amplitudes decrease. These effects may be seen in all those intervals in all other positions of the gauges. It may be seen also that there are amplitudes that grow very fast with distance. This is due to the non-linear effects that result in contraction. To obtain a more detailed insight the initial intervals are zoomed in Fig. 5. From these graphs can be seen how the changes move inside the regular part when the train moves along the flume. The comparison of the measurements at the reference gauge $S1$ with smooth intervals of growth and decay with the measurements at succeeding gauges up to $S7$ shows the extent of the transformations.

There is, of course, the problem of how the transformation is effected by the choice of procedure that defines the way the waves grow and decay. To study this problem one has to look at a suitable model that reproduces the experiments and

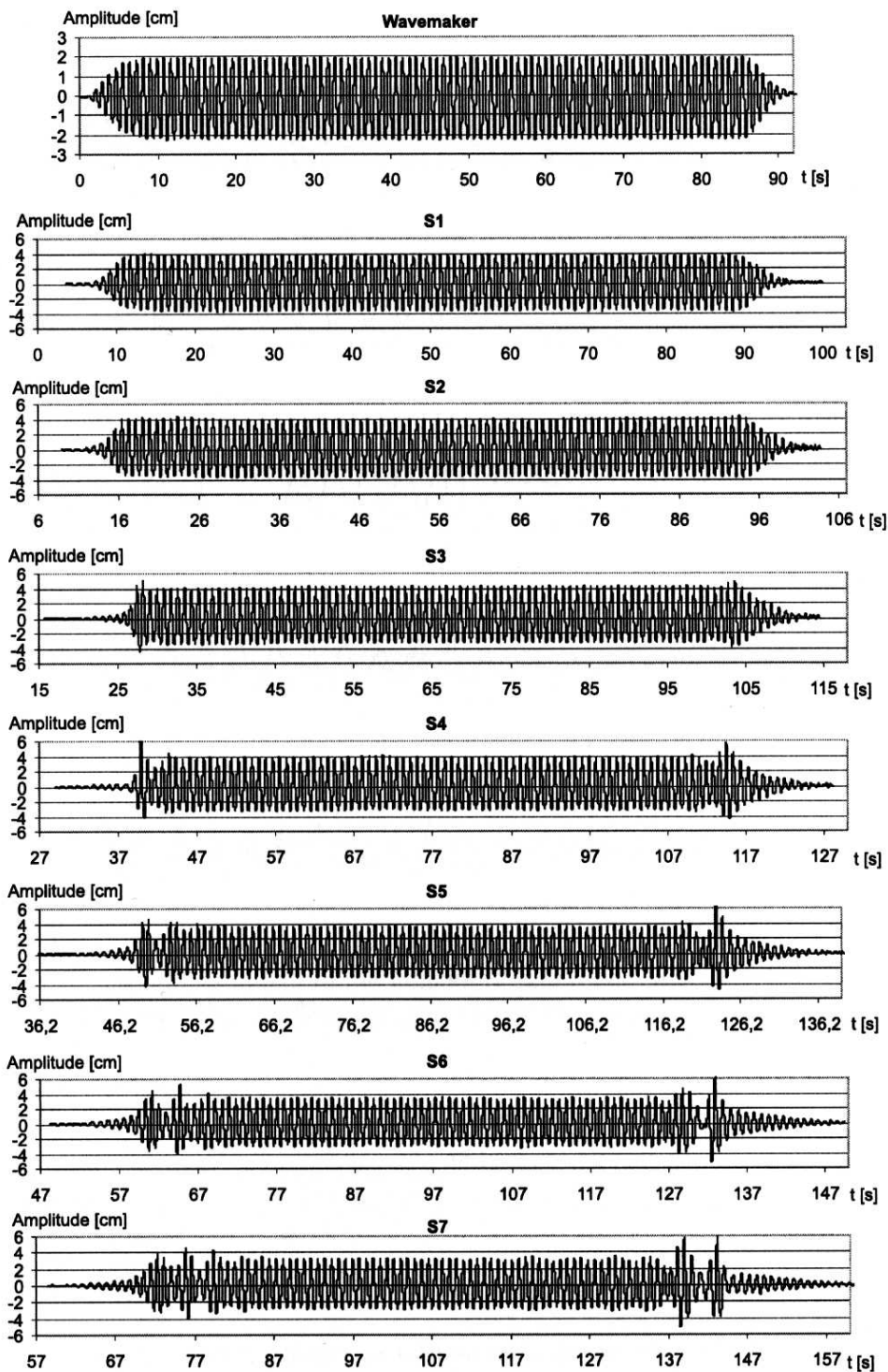


Fig. 4. The transformation of wave profiles along the propagation way

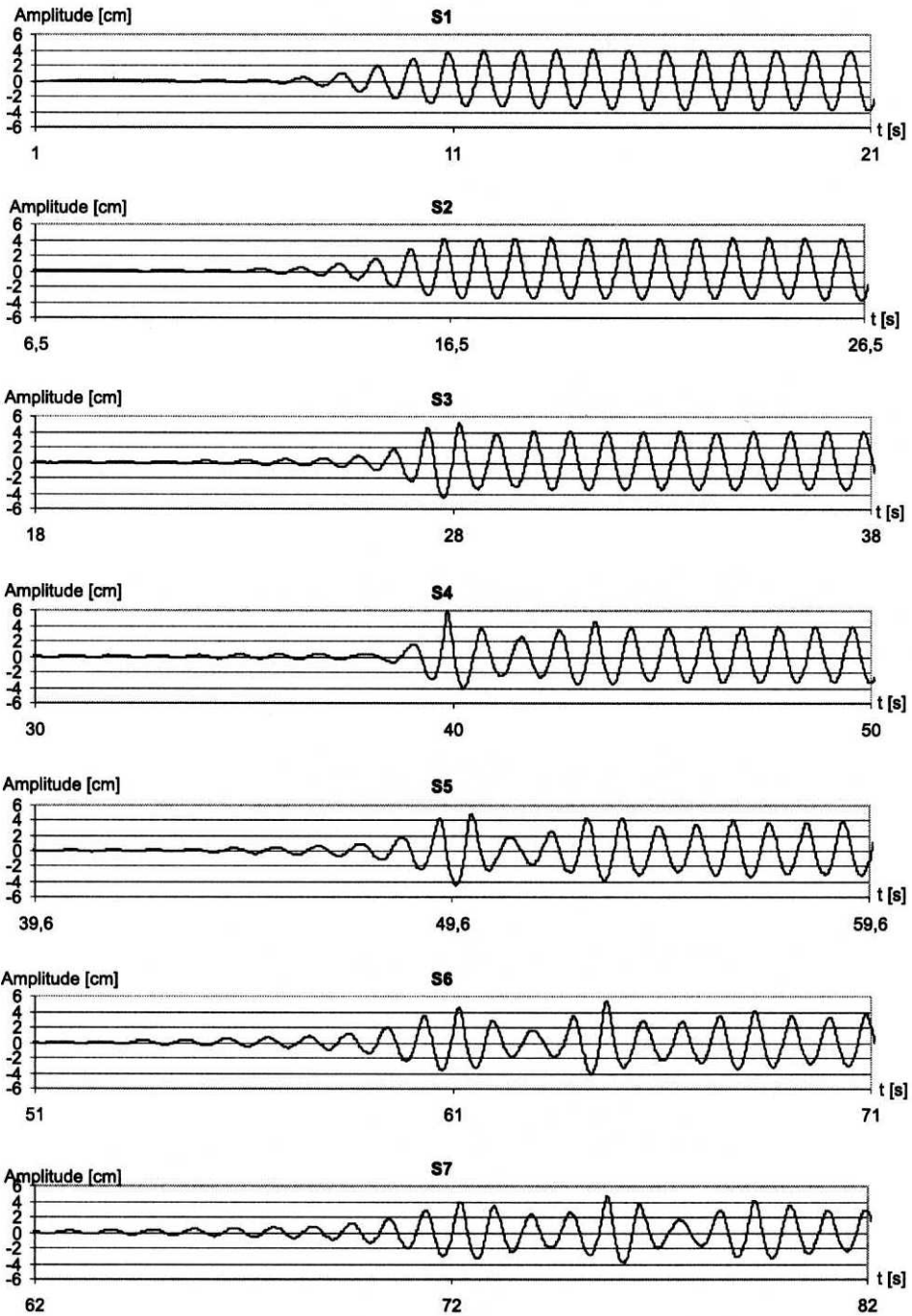


Fig. 5. The initial intervals of the recorded wave profiles depicted in Fig. 4

may be used to find a set of solutions with changed parameters of growth and decay. At this preliminary stage the non-linear Schroedinger equation was used and the numerical solution for the amplitudes is compared with the experimental data for a measured shorter wave train.

A computer programme was prepared for the solution of a special case of the Schroedinger equation. It was based on the paper by Pelinovski and others (1988). A short outline of the procedure is presented.

Let us introduce the following transformation of variables and its inverse

$$\begin{bmatrix} \xi \\ \tau \end{bmatrix} = \begin{bmatrix} 1 & -v_g \\ 0 & 1 \end{bmatrix} \begin{bmatrix} x \\ t \end{bmatrix}, \quad \begin{bmatrix} x \\ t \end{bmatrix} = \begin{bmatrix} 1 & v_g \\ 0 & 1 \end{bmatrix} \begin{bmatrix} \xi \\ \tau \end{bmatrix}. \quad (22)$$

In the new variables the differential equation (5) reduces to

$$iA_{,\tau} + \alpha A_{,\xi\xi} - \beta |A|^2 A = 0. \quad (23)$$

The transformed differential equation in the complex amplitude A as a function of ξ and τ is simpler. We have to take as the initial state, the measurements at the reference gauge S1.

Assume that for the time $\tau = 0$ the complex amplitude $A(\xi, 0)$ is known from the experimental data. Intervals with zero values have to be added in front and behind the time series of the estimated amplitude. A periodic function is formed with the length l .

A finite Fourier transform is calculated according to the formula

$$F(\tau, s) = \frac{1}{l} \int_0^l A(\tau, \xi) \exp(-is2\pi\xi/l) d\xi, \quad (24)$$

where s is a set of integers from the interval $[-n, n]$ and n are the Nyquist frequencies corresponding to half of the number of points considered in the interval of length l . The inverse transformation is given by the formula

$$A(\tau, \xi) = \int_0^l F(\tau, s) \exp(i\xi 2\pi s/l) ds. \quad (25)$$

Expressions (24) and (25) are written in the form of Fourier transforms. When s are integers the relations go over to Fourier series.

Let us introduce the notation

$$F_{|A|A}(\tau, s) = \frac{1}{l} \int_0^l |A(\tau, \xi)|^2 A(\tau, \xi) \exp(-is2\pi\xi/l) d\xi, \quad (26)$$

and take the Fourier transform of the differential equation (23). It follows that

$$i \frac{\partial}{\partial \tau} F(\tau, s) + \alpha s^2 F(\tau, s) + \beta F_{|A|^2 A}(\tau, s) = 0. \quad (27)$$

In the differential equation (27) the first two terms are linear and the third term is unknown. For the initial state the complex amplitude is known and the Fourier transforms appearing in the third term, according to Eq. (24) can be calculated. Now we may consider small steps $\Delta\tau$, apply numerical integration by the trapezoidal rule and use estimation in steps and iterations to obtain a good approximation. It should be noted that when the parameter β is equal to zero the linear Schroedinger equation results and the Eq. (27) goes over to an ordinary linear differential equation in the unknown Fourier transform. This differential equation has a simple solution and when the third term is known the variation of the constant of integration has to be considered to obtain a solution of the non-homogenous differential equation. These transformations lead to a description by an integral equation that is based on the Schroedinger differential equation. The iteration procedure described in the above mentioned paper is highly effective.

The results are depicted in Fig. 6. It may be seen that the solution reproduces the behaviour and confirms the Schroedinger differential equation as a suitable model to obtain an insight into the transformation.

Another problem is the stability of motion of the regular part. The regular wave is a solution of the problem, but if there are discrepancies from the perfect wave, some forms of the discrepancies may grow and thus the wave may become unstable. If there is more "noise" in the flume the loss of stability may be more easily observed. The measurements depicted in Figs. 4 and in 6 show that groups begin to appear also in the regular part of the train at the last gauges.

5. The Stability of a Regular Wave Train

In both theory and experiments, small modulations in the form of wave groups are introduced in the initial state, then the wave profiles are measured by means of propagation along the flume. Such experiments are depicted in Fig. 7. The modulation of the piston motion corresponded to six waves in a group and amplitudes equal to 5% ($c_r = a_m/a_0 = 0.05$) of the basic amplitude. The graphs clearly illustrate the changes in the groups along the flume. The motion is not stable if the infinitesimal modulations grow. The large changes that are seen at the end part of the flume correspond to finite displacements and can not be considered as superposition of infinitesimal displacements. The Schroedinger equation can give only a simplified description, in full description finite transformations have to be considered. Fig. 8 presents the results of measurements with the same wave parameters, but with amplitudes of modulations increased to 15%. It can be seen

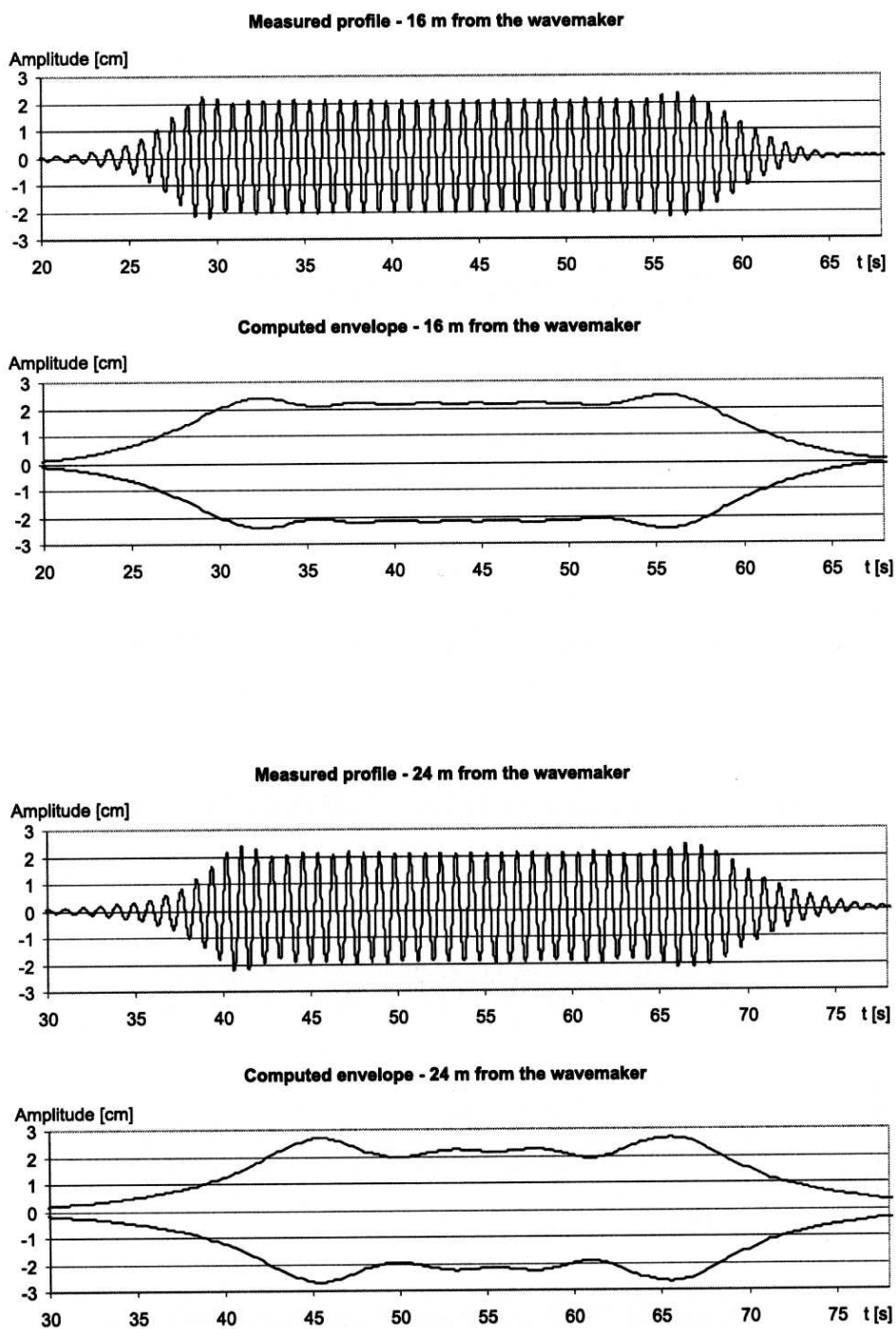


Fig. 6. The comparison of recorded and computed envelopes at the distances $x = 16$ m and $x = 24$ m from the wavemaker

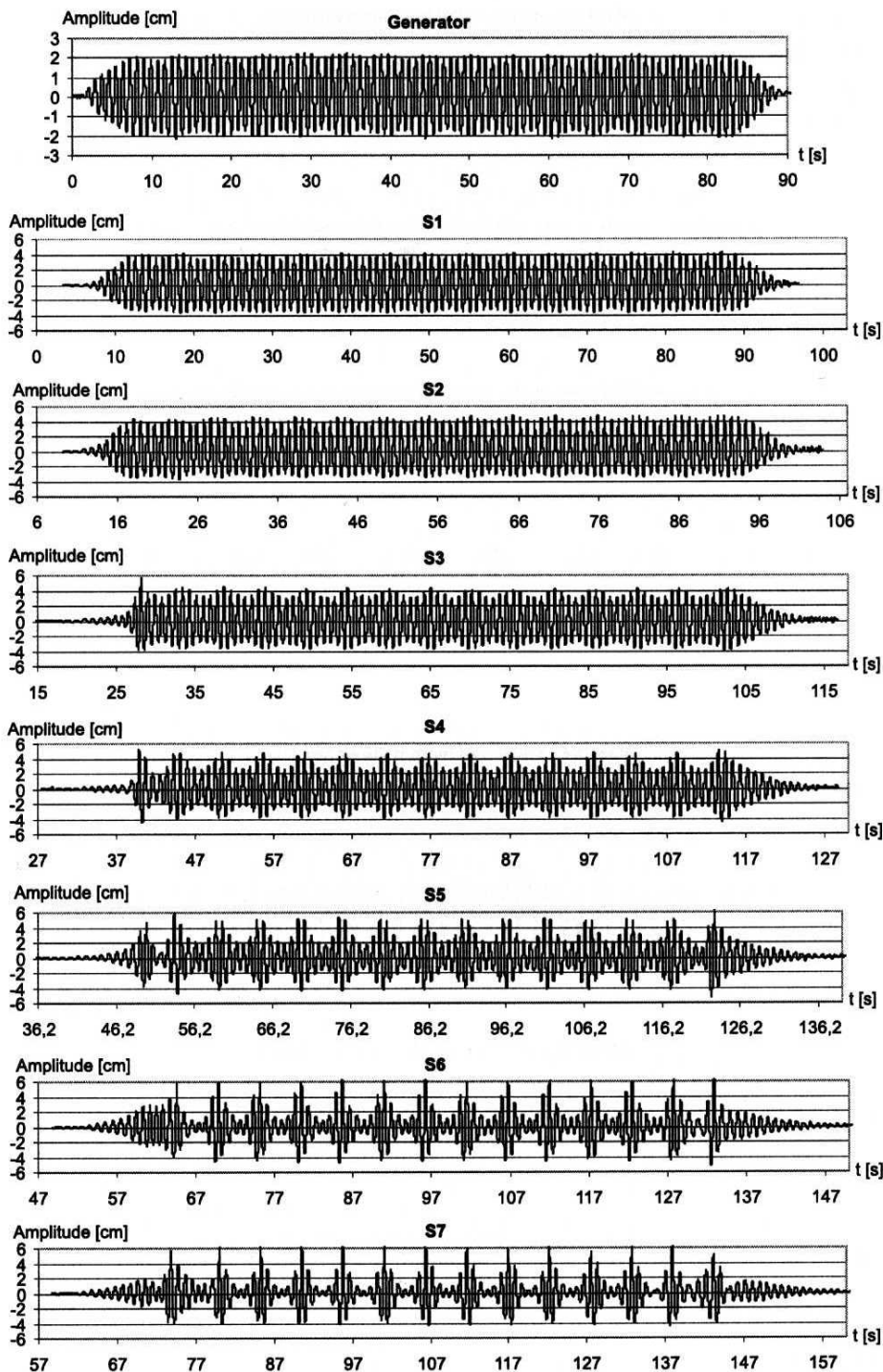


Fig. 7. The transformation of wave profiles along the propagation way. Modulated motion of the wavemaker, $c_r = 0,05$

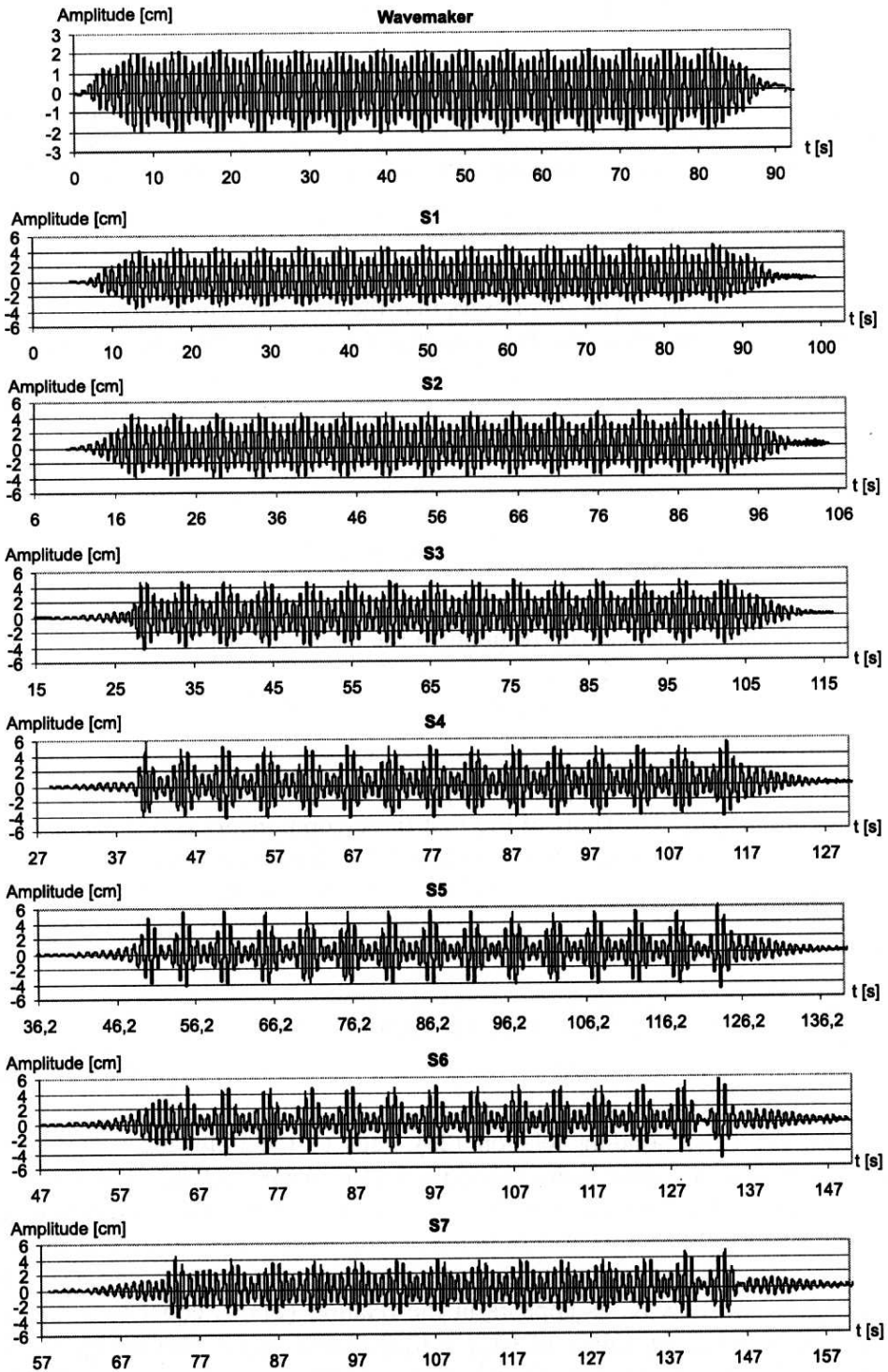


Fig. 8. The transformation of wave profiles along the propagation way. Modulated motion of the wavemaker, $c_r = 0.15$

that the gauge $S5$ presents the groups in the most advanced form and then in the following gauges ($S6$, $S7$) the modulations decrease. For the case of 30% initial amplitudes modulation the development of groups is more restrained (Fig. 9). These graphs show clearly that the influence of largeness of initial displacements is important.

In Fig. 3 the region of instability is shown and the influence of the wave numbers in the group on the growth rate is stressed. In Fig. 10 (as measured at $x = 26.67L_l = 32$ m) and Fig. 11 (as measured at $x = 40L_l = 48$ m) the results of measurements with 5% modulations are presented for different numbers of waves n_T in the groups. The theory says that the development of groups is fastest with groups of 5.36 waves. At distances equal to $x = 26.67L_l$ and $x = 40L_l$ the modulations with 6 wave periods yield the best developed wave groups.

Following the relation (21) the surface elevations at gauges $S2$ and $S3$ as functions of time can be presented by the following expressions

$$Z_2 = \sum_{j=1}^{j=4} (a_{2j} + id_{2j}) \exp(-i\omega_{2j}t), \quad Z_3 = \sum_{j=1}^{j=4} (a_{3j} + id_{3j}) \exp(-i\omega_{3j}t). \quad (28)$$

The angular frequencies correspond to the elements of the row matrix

$$\Omega = [\omega_d - \omega_d/n_T, \omega_d, \omega_d + \omega_d/n_T, 2\omega_d], \quad (29)$$

where, in the case considered the number of waves n_T in a group is six. The method of least squares is applied for approximation of the measured time series by the relation (28). The sums of the first three components and sums of all the estimated components are depicted in Fig. 12. Calculations showed that for the two gauges considered the angular frequencies are the same and thus, in view of the expression (21), the phases of the surface elevations at $S3$ may be expressed in terms of the ones at $S2$ as

$$\text{angle}(Z_{3j}) = \text{angle}\{Z_{2j} \exp[iK_{pj}(x_3 - x_2)]\}, \quad (30)$$

where x_3, x_2 are the distances from the generator to gauges $S3$ and $S2$, and K_{pj} are the wave numbers corresponding to the components. Comparison of the relation (30) with the corresponding relation (28) leads to the following values of the elements of the row matrix $\mathbf{K}_p = [3.580, 5.116, 6.648, 8.078]$. The length of the dominant wave component is $L_2 = 2\pi/K_{p2} = 1.23$ m while according to the expression (10) it should be 1.25 m. These values based on experimental data are very close. It is easy to verify that the difference between $K_{p2} - K_{p1}$ and $K_{p3} - K_{p2}$ is negligible and thus K , as appears in the relation (21), is equal to 1.533. The difference between the values of $(K_{p1} + K_{p3})/2$ and K_{p2} is also negligible. The ratio of K/K_{p2} is very close to 1/3 and thus the number considered in time is twice

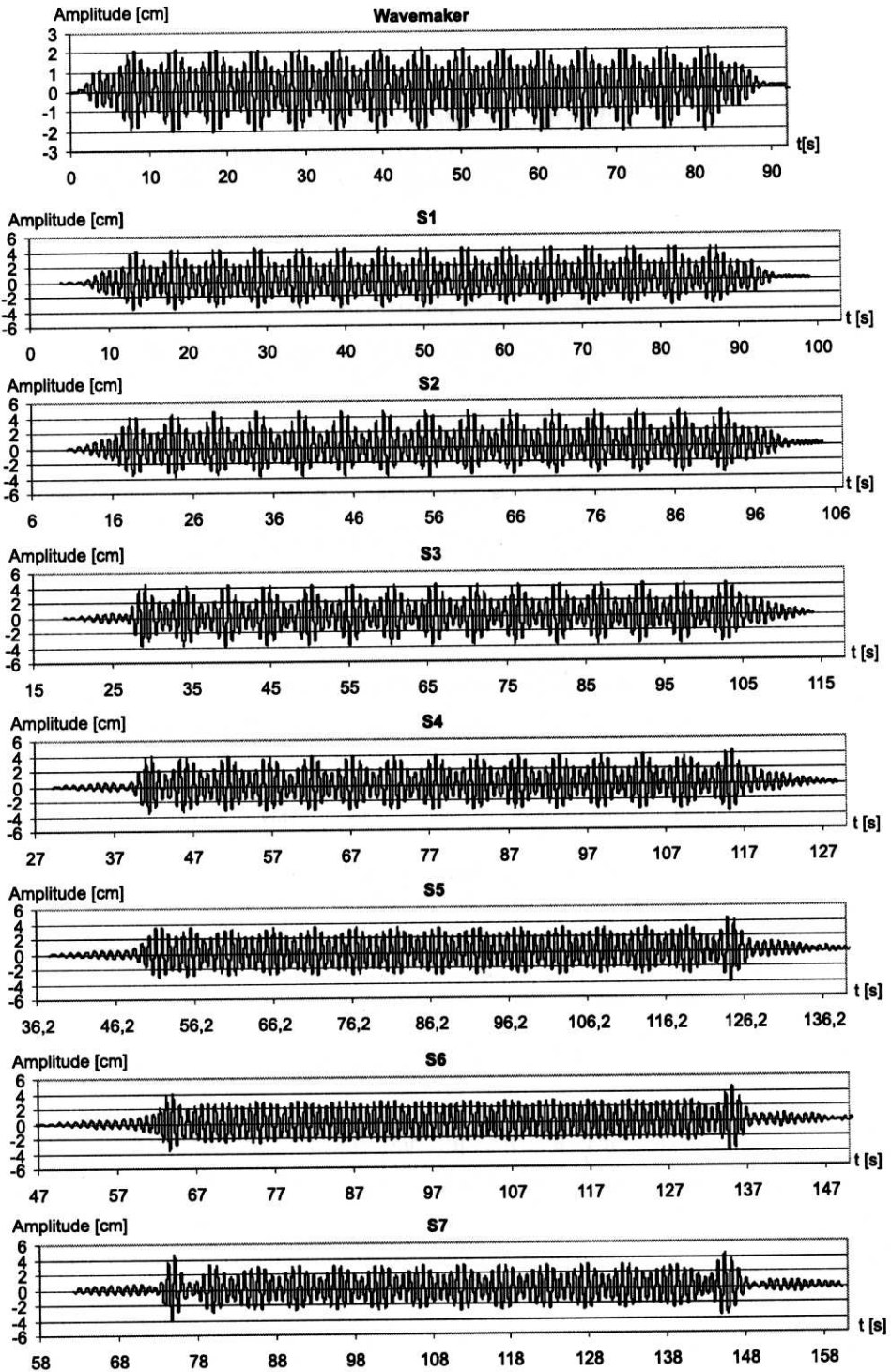


Fig. 9. The transformation of wave profiles along the propagation way. Modulated motion of the wavemaker, $c_r = 0,30$

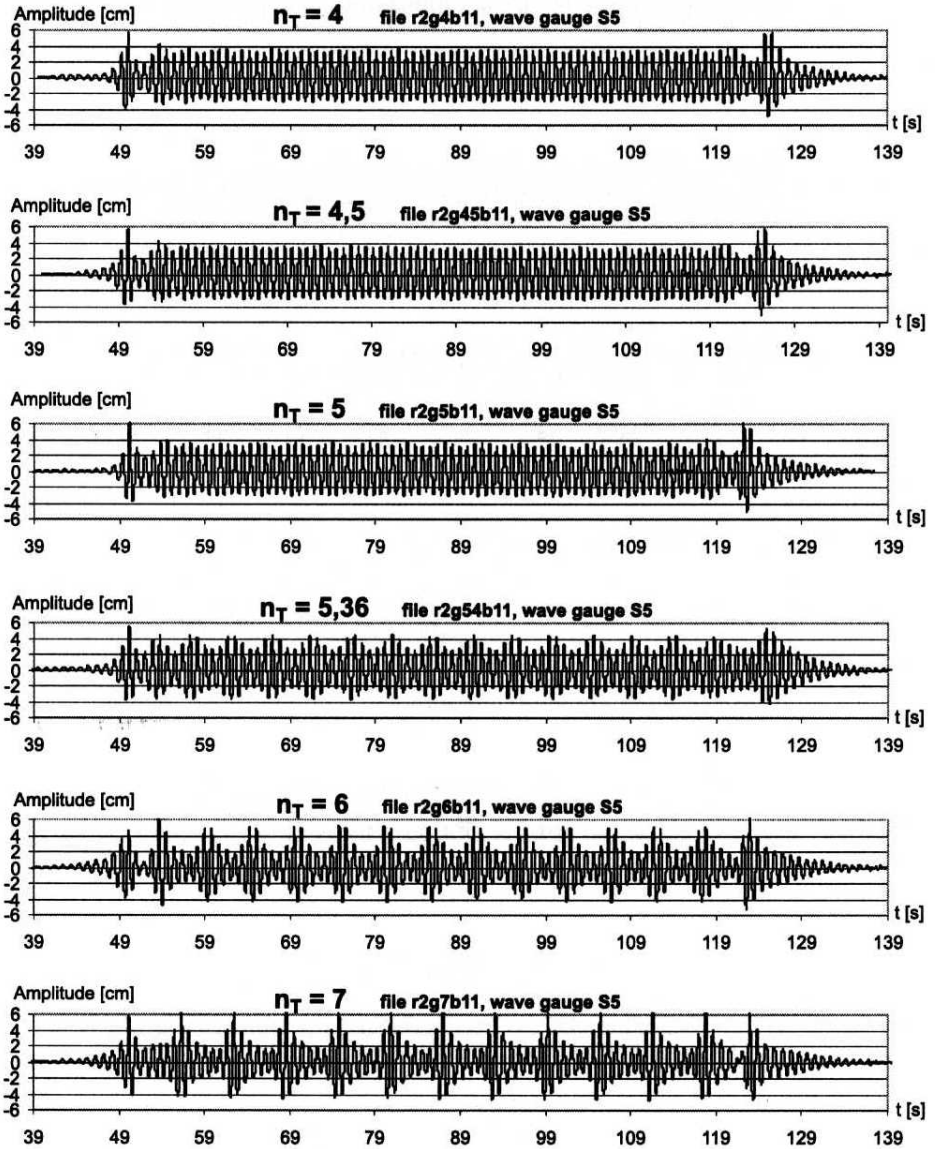


Fig. 10. The transformation of wave profiles dependent on number of waves n_t in groups at modulations $c_r = 0.05$ as measured at the position S5 ($x = 26.67L_l$)

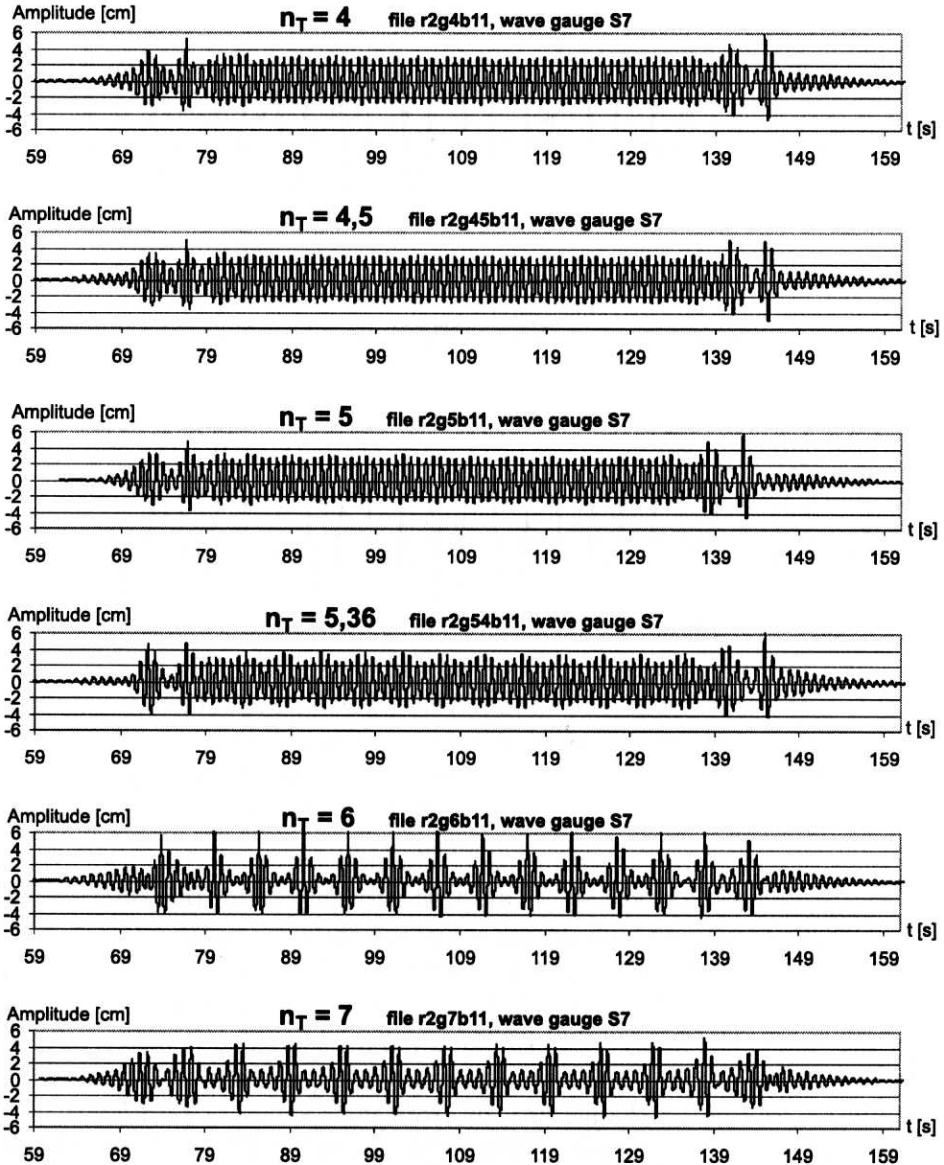


Fig. 11. The transformation of wave profiles dependent on number of waves n_t in groups at modulations $c_r = 0.05$ as measured at the position S7 ($x = 40L_l$)

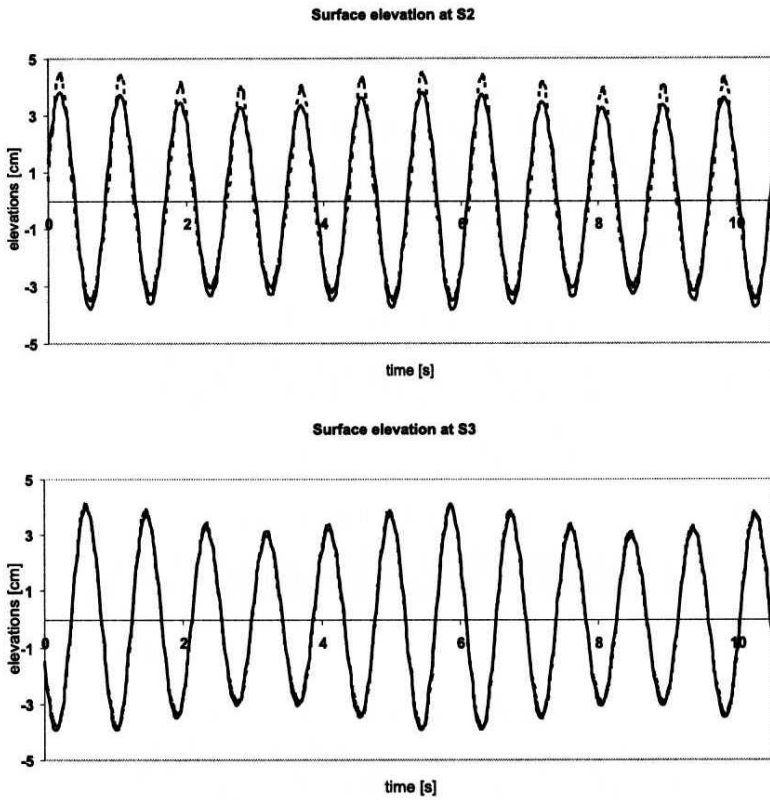


Fig. 12. The sum of three components $\omega_d - \Delta\omega$, ω_d , $\omega_d + \Delta\omega$ (solid lines) and four components ($2\omega_d$ added, dashed lines). At S3 the component $2\omega_d$ is equal to zero

the number of waves considered in space. The non-linear Schroedinger equation describes the behaviour correctly. It must be stressed that in this transformation the modifications increase with distance, but remain very small.

In Fig. 13 the surface elevation as a function of distance from the generator is plotted. The co-ordinates of the surface are calculated as the real part of the sum of the first three terms with estimated parameters. The depicted envelopes correspond to the absolute values of the complex expressions. It is assumed that the amplitude and phase change linearly from their values at position S2 to S3. Comparison of Fig. 12 with Fig. 13 clearly shows the difference of behaviour of the groups in time and space.

Now let us look at the behaviour based on measurements far from the generator. To get an insight of the behaviour we measured the surface elevations with 20 cm spacing by a set of seven gauges. The measurements were repeated with the set moved to new positions. To control the positions the last gauge corresponded with the first in the preceding experiment. The corresponding measurements should

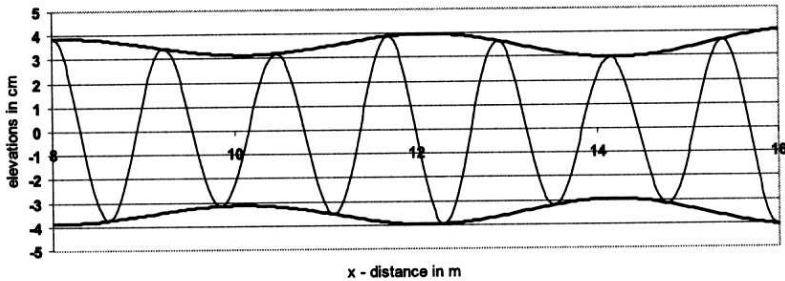


Fig. 13. Surface elevation as the function of x calculated on the basis of three components of the Fourier series at S_2 ($x = 8$ m) and S_3 ($x = 16$ m) and the corresponding envelopes

have the same values. There were differences. Thus, the measured time series at positions S_k for $k = 1, 2, \dots$ with distances from the generator $x_k = 40 + (k - 1) 0.20$ covered the interval 40 m up to 49.6 m from the generator. The same time interval of twelve waves (two wave groups) was chosen to obtain an approximate description for all the positions of the gauges by addition of terms as given by the expression (28). The absolute values of the components with angular frequencies corresponding to the matrix (30) are depicted in Fig. 14. The corresponding phases are shown in Fig. 15. It is worthwhile noting that the straight-line approximation for the values of phases is very good. The straight-line approximations for the absolute values is not as good, but it shows that the absolute value of the component with the dominant frequency decreases, while the amplitudes of components corresponding to the side bands increase.

The slopes of the phases of components correspond to their wave numbers. The experiments indicate that the wave numbers do not change within the considered interval. The straight-line-approximation yielded the following row matrix of slopes of the components: $\mathbf{K}_A = [3.520, 5.00, 6.540, 8.058]$. The comparison of this matrix with the matrix \mathbf{K}_P calculated on the measurements at S_2 and S_3 shows that there are differences in the values of corresponding elements but the differences are not large.

The position of the free surface estimated as the sum of three components based on the amplitudes (Fig. 14) and phases (Fig. 15) within a straight-line approximations are depicted in Fig. 16 by a solid line. The envelopes correspond to the absolute values. The dashed lines illustrate the free surface calculated with the time shifted by half of the dominant period. The number of waves in a group in space does not exactly equal three as it should be within the simplified analysis. Still the simplified analysis furnishes a reasonable estimate.

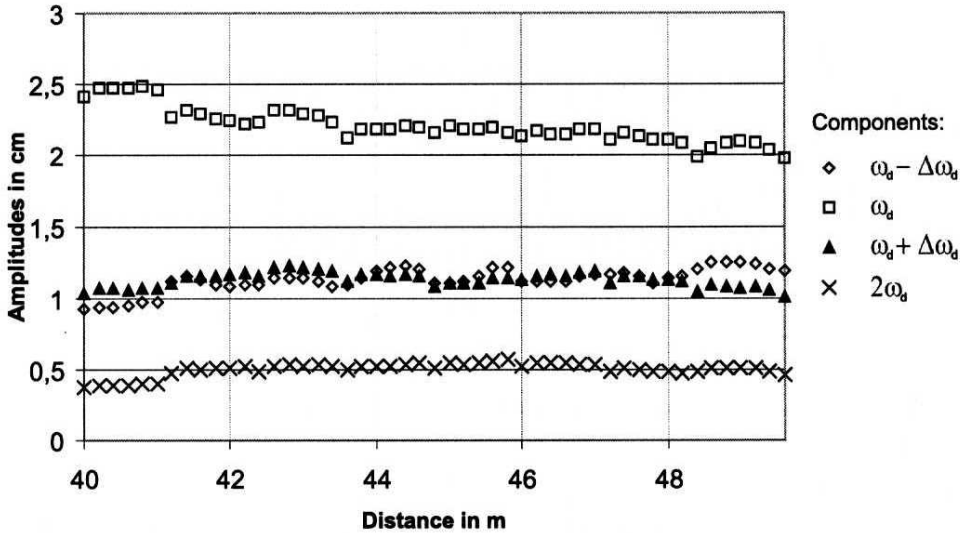


Fig. 14. Experimental amplitudes of components as functions of distance x

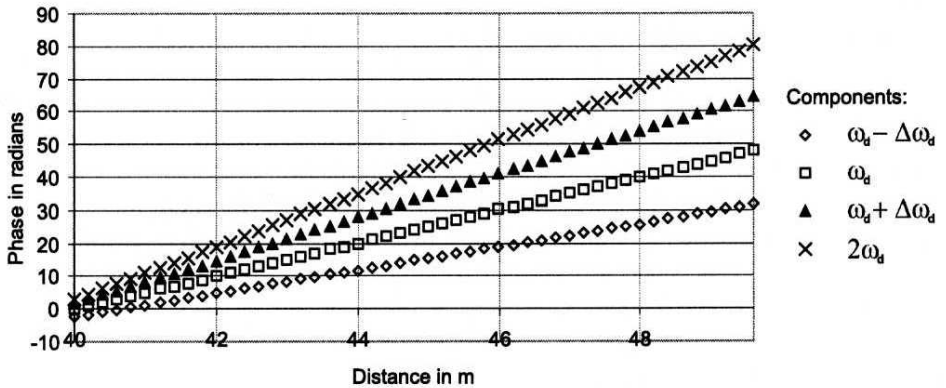


Fig. 15. Phases of components as functions of distance x

An example of wave train as an interval of the measured time series of length corresponding to five groups with six waves in each and the corresponding amplitudes of the Fourier Series are shown in Fig. 17. In the stability analysis the dominant frequency ω_d and the two important side band frequencies $\omega_d - \Delta\omega_d$, $\omega_d + \Delta\omega_d$ are considered. All the other components are neglected. It is worthwhile noting that the Stokes double frequency component goes over to a

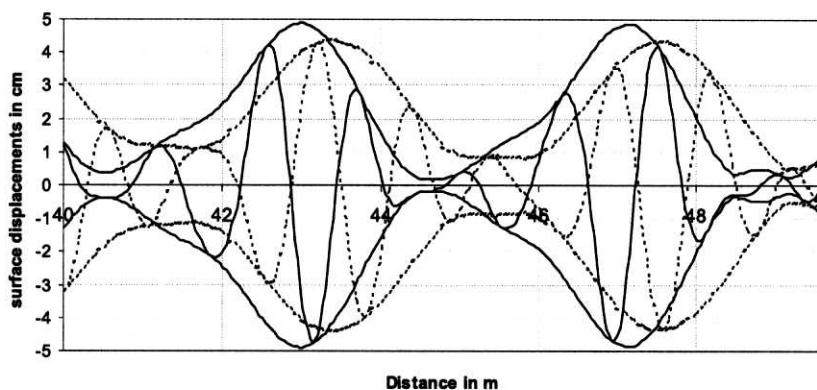


Fig. 16. The estimated wave profiles and their envelopes at a fixed time – solid lines and shifted in time by $T_d/2$ – dashed lines

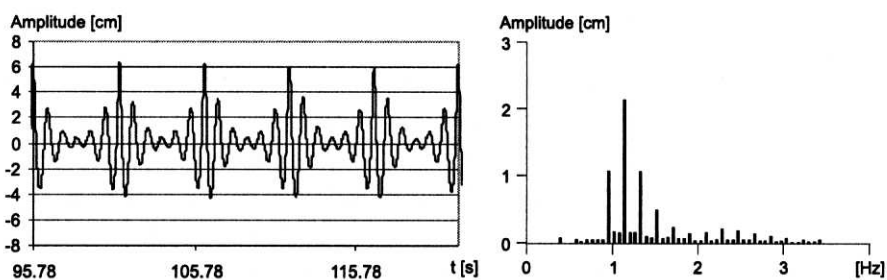


Fig. 17. An example of an interval of the measured time series at the position $S7$ ($x = 48$ m) of five groups length with six waves in each and the corresponding amplitudes of Fourier Series components

set of components with small amplitudes. It is obvious that three components can not in detail represent a process that has so many components as is seen in the Fourier Series.

6. Conclusions

1. The deep-water wave trains generated by piston type wavemaker have been investigated. The behaviour is similar to that observed by Yuen and Lake (1982) with waves produced by a paddle type generator in a wave flume with smaller dimensions.
2. For the case of wave trains generated with a long interval of regular waves between the intervals of growth and decay the transformations along the flume start from the ends of the trains. The groups created intrude into the

- middle part of regular waves. The choice of a method of generation has a significant influence on the wave group phenomenon.
3. As in standard procedures, initial modulations are introduced to discuss the stability problem. The ratio of the amplitudes of the modulation and the regular wave a_m/a_0 is an important parameter. Even a small value $a_m/a_0 = 0.05$ leads to very fast growth of groups and thus the regular wave is not stable.
 4. The non-linear Schroedinger equation describes the stability behaviour well. The experiments with different numbers of waves in a group considered in time confirm in general the theoretical regions of instability (Fig. 4). However, our experiments indicate that the rate of growth of modulations depends on the number of waves in a group and does not correspond strictly with the theoretical value (Fig. 10, Fig. 11). Thus the Schroedinger equation does not describe the real behaviour perfectly.
 5. Experiments with large initial modulations show that there are substantial differences in behaviour. The intensities of modulations change along the path of wave propagation. In the vicinity of the wavemaker the modulations increase and then decrease along the way of propagation. To describe these phenomena it is necessary to consider finite initial modulations.
 6. The Fourier series that represent the groups in measured wave trains (Fig. 17) indicates that the Schroedinger solution does not describe the behaviour to perfection. For the waves with initial modulations with n waves in a group considered in time and the dominant frequency ω_0 , there is a sequence of important frequencies corresponding to the multiples of $\omega_0/6$. In the Schroedinger equation theory, the second Stokes' harmonic is disregarded. The measurements show that there are two large frequencies corresponding to the Benjamin Feir side bands and they are accompanied by many terms with smaller, but significant amplitudes. The neighbourhood of the second Stokes' harmonic is covered by these terms.

References

- Benjamin T. B. (1967), Instability of Periodic Wavetrains in Non-linear Dispersive Systems, *Proc. R. Soc. London, Ser. A*, Vol. 299, 59–75.
- Benjamin T. B., Feir J. E. (1967), The Disintegration of Wavetrains on Deep Waters. Part 1. Theory, *J. Fluid Mech.*, Vol. 27, 417–430.
- Chereskin T. K., Mollo-Christensen E. (1985), Modulational Development of Non-linear Gravity-Wave Groups, *J. Fluid Mech.*, Vol. 151, 337–365.
- Hasimoto H., Ono H. (1972), Non-linear Modulation of Gravity Waves, *J. Phys. Soc. Jpn*, Vol. 33, 805–811.
- Hasselmann D. E. (1979), The High Wave Number Instabilities of a Stokes Wave, *J. Fluid Mech.*, Vol. 93, 491–500.
- Lake B. M., Yuen H. C. (1977), A Note on Some Non-linear Water Wave Experiments and the Comparison of Data with Theory, *J. Fluid Mech.*, Vol. 83, 75–81.

- Lake B. M., Yuen H. C., Rungaldier H., Ferguson W. (1977), Non-linear Deep-Water Waves: Theory and Experiment. Part 2. Evolution of a Continuous Wave Train, *J. Fluid Mech.*, Vol. 83, 49–74.
- Lighthill M. J. (1965), Contributions to the Theory of Waves in Non-linear Dispersive Systems, *J. Inst. Math. Appl.*, Vol. 1, 269–306.
- Pelinovsky E. N., Stiepanianc J. A., Filienkov S. E. (1988), Soliton Type Modulations in Dispersive Waves (in Russian), *Internal report Department of Theoretical Physics*, Gorki University.
- Shemer L., Jiao Haying, Kit E. (1988), Experiments on Non-linear Wave Groups Shoaling in a Tank, *Proc. of Coastal Engineering 1988*, ASCE, Vol. 2, 645-655.
- Skjelbreia L. (1959), *Gravity Waves. Stokes' Third Order Approximation. Tables of Functions*, Richmond Calif.; Council on Wave Research.
- Sobierajski E. (1999), Testing of Wave Processes in the New Flume of the Institute of Hydro-Engineering, *Internal report*, (in Polish).
- Stansberg C. T. (1992), On Spectral Instabilities and Development of Non-linearities in Propagating Deep-water Wave Trains, *Proc. of Coastal Engineering, 1992*, ASCE, Vol. 1, 658–671.
- Werhausen J. V., Laitone E. V. (1960), Surface Waves, [in] *Encyclopedia of Physics*, Springer Verlag, Berlin, Goettingen, Heidelberg.
- Wilde P., Wilde M. (2001), On the Generation of Water Waves in a Flume, *Archives of Hydro-Engineering and Environmental Mechanics*, No. 4, 69–83.
- Witham G. B. (1974), *Linear and Non-linear Waves*, Wiley, New York.
- Yuen H. C., Lake B. M. (1982), Non-linear Dynamics of Deep Water Waves, *Advances in Applied Mechanics*, Vol. 22, 67–229.
- Zacharov V. E. (1968), Stability of Periodic Waves of Finite Amplitude on the Surface of a Deep Fluid, *Sov. Phys. J. Appl. Mech. Tech. Phys.*, 4, 86–94.